RAPID COMMUNICATIONS

PHYSICAL REVIEW B VOLUME 35, NUMBER 13 1 MAY 1987

Spectroscopy of glassy systems with a relaxation-time distribution: Application to Brillouin scattering on $Rb_{0.65}(NH_4)_{0.35}H_2PO_4$

Eric Courtens
IBM Research Division, Zurich Research Laboratory, 8803 Rüschlikon, Switzerland

René Vacher
Laboratoire de Science des Matériaux Viteux, Université de Montpellier II, F-34060 Montpellier, France
(Received 2 February 1987)

Glassy systems often have a broad distribution of relaxation times difficult to determine experimentally. A new approach for spectrum analysis, which could find considerable application, is described. It is based on the expansion of a relaxation function in the logarithm of the frequency, and applied successfully to Brillouin data on $Rb_{0.65}(NH_4)_{0.35}H_2PO_4$, demonstrating the physical interpretation of the experimental expansion coefficients.

There is considerable current interest in the spectroscopy of frustrated systems forming glasses at low tempertures.[1] One of their universal properties appears to be that their dynamics is characterized by a broad distribution of relaxation times τ.[2] In the case of spin glasses, it has become customary to describe results by a distribution $g(\tau,T)$, normalized to 1 upon integration over $d\ln\tau$.[3-5] In terms of g, one defines a relaxation function $\kappa(\omega,T)$, where ω is the measuring frequency and T the temperature,

$$\kappa(\omega,T)\equiv\kappa_R+i\kappa_I=\int_0^\infty \frac{g(\tau,T)d\ln\tau}{1-i\omega\tau} \ . \tag{1}$$

Recently, a similar approach was taken for $Rb_{1-x}(NH_4)_xH_2PO_4$ (RADP) structural glases,[6] in which there is random competition between the ferroelectric (FE) ordering of RbH_2PO_4 and the antiferroelectric one of $NH_4H_2PO_4$.[7] Its microscopic origin has been explained elsewhere.[8] The frustration leads to a disordered freezing of polarizations for intermediate ammonium concentrations x, $0.22\lesssim x\lesssim 0.74$.[9] As those crystals are also piezoelectric, they exhibit a linear coupling between the polarization and a number of acoustic modes. This leads to characteristic Brillouin spectra, as explained for the concentration $x=0.35$ in Ref. 10, hereafter referred to as I. In I, the spectra were interpreted using (1) where, on the basis of previous knowledge,[6] the simplest approximation of a rectangular distribution for $g(\tau,T)$ was made.

An alternative approach is presented here. It allows one to obtain information on $g(\tau,T)$ from the spectra, independently from an assumption on the specific functional form of the latter. This new method of analysis may find considerable application, and its use may extend beyond RADP and, in fact, beyond Brillouin scattering and the specific case of piezoelectrically coupled spectra. It is applied here to the $x=0.35$ spectra already fitted in I. In that case, the information on $g(\tau,T)$ is interpreted in terms of a scaling function $f(E)$, where E is related to τ by a Vogel-Fulcher (VF) ansatz[11]

$$E=(T-T_0)\ln(\tau/\tau_0) \ . \tag{2}$$

Here, T_0 is the VF freezing temperature, and τ_0 an inverse attempt frequency.

The spectra to be analyzed were obtained on the $T_1[100]$ acoustic mode,[10] which is the soft one for the FE transition of KH_2PO_4.[12] The corresponding bare or uncoupled phonon frequency is called ω_a. This phonon couples linearly to the polarization. The susceptibility of the latter,

$$\chi(\omega,T)=\chi_B+\chi_0(T)\kappa(\omega,T)$$

is the superposition of an adiabatic background χ_B, which is small and can be taken as constant, with an isothermal contribution $\chi_0(T)$ weighted by the relaxation function. This model is sufficient to describe the Brillouin spectra, as shown in I. The general expression for the spectral profile is[10]

$$I(\omega,T)\propto\frac{kT}{\pi\omega}\frac{\kappa_I p^2}{\chi_0 h^2}\frac{[1+\Upsilon(1-\omega^2/\omega_a^2)]^2}{\{\kappa_R+(\chi_B/\chi_0)-Q[1+(\chi_B/\chi_0)][1-(\omega^2/\omega_a^2)]\}^2+\kappa_I^2} \ , \tag{3}$$

where κ_R and κ_I are defined in (1). It should be noted that (3) applies to any distribution $g(\tau,T)$, including a simple Debye relaxation of characteristic time $\bar{\tau}$, $g(\tau)=\tau\delta(\tau-\bar{\tau})$, where δ is the Dirac function.

In addition to κ, the profile depends on χ_B/χ_0, Q, Υ, and ω_a. Those parameters were discussed in I, where it was shown that (i) the ratio χ_B/χ_0 can be taken from the dielectric data, (ii) $Q(T)$ for this mode can be extracted from a comparison of the free and clamped dielectric constants, (iii) the profile depends only weakly on Υ, a dimensionless and nearly T-independent quantity which can be well estimated from the high-T intensities, and (iv) ω_a can be extrapolated from the high-T region using a Debye approximation to account for lattice anharmonicity.

It must be appreciated that although evidence for a distribution $g(\tau,T)$ does appear in many measurements, g is

seldom sufficiently known to allow for direct calculation of $\kappa(\omega,T)$ using (1). This is a general difficulty in the evaluation of relaxation data in glass, which should be faced rather than ignored.[13] As parameters χ_B/χ_0, Q, Υ, and ω_a are well determined by a combination of dielectric and high-T Brillouin data, they are fixed in (3), allowing fitting directly for κ_R and κ_I at temperatures where elastic and polarization fluctuations strongly couple. However, the frequency dependence of κ is of some importance in determining the exact spectral profile. As $g(\tau,T)$ is broad in $\ln\tau$, it results that $\kappa(\omega,T)$ is broad in $\ln\omega$. Thus, an expansion in $\ln\omega$ about a central value $\bar{\omega}$ near ω_B is adequate in the frequency range of the Brillouin spectra. Hence, we use in (3),

$$\kappa_R(\omega,T)=\kappa_R(\bar{\omega},T)-\frac{2}{\pi}\kappa_I(\bar{\omega},T)\ln(\omega/\bar{\omega}) -\frac{1}{\pi}m(\bar{\omega},T)[\ln(\omega/\bar{\omega})]^2+\cdots , \quad (4a)$$

$$\kappa_I(\omega,T)=\kappa_I(\bar{\omega},T)+m(\bar{\omega},T)\ln(\omega/\bar{\omega})+\cdots , \quad (4b)$$

where

$$m(\bar{\omega},T)\equiv(\partial\kappa_I/\partial\ln\omega)_{\omega=\bar{\omega}} . \quad (4c)$$

The expansion (4a) is consistent with (4b), given the *local* Kramers-Kronig relation

$$\kappa_I(\omega,T)=-(\pi/2)\partial\kappa_R(\omega,T)/\partial\ln\omega ,$$

known to apply when $g(\tau,T)$ is broad in $\ln\tau$.[3] This relation was verified experimentally for RADP with $x=0.35$ at audio frequencies.[6]

It should be noted that κ_I in (4b) does not exhibit explicitly the usual linear dependence on ω at small ω imposed by causality.[14] This unusual feature of glasses, which applies over a broad range of intermediate frequencies, is a spectacular consequence of the broad distribution of relaxation times. It produces a dynamical central peak, which might have a narrow dip near $\omega=0$, the latter so far unobserved. This peak, already noted in I, is essentially caused by the κ_I/ω prefactor in (3).

It is apparent from (3) that $\kappa_R(\bar{\omega},T)$ and $\kappa_I(\bar{\omega},T)$ are mainly determined by the position and width of the Brillouin peaks, respectively. These two coefficients are sufficient to describe the main features of the spectra, including the dynamical central peak over the limited frequency range of its measurement. However, the fine details of the line shape, in particular between ω_B and the lowest measurable frequency $\omega_{\min}$, may require the additional expansion coefficient $m(\bar{\omega},T)$. In terms of integrals over g, those coefficients are

$$\kappa_R(\bar{\omega},T)=\int_0^\infty\frac{g(\tau,T)d\ln\tau}{1+\bar{\omega}^2\tau^2}\simeq 1-\int_{1/\bar{\omega}}^\infty g(\tau,T)d\ln\tau, \quad (5a)$$

$$\kappa_I(\bar{\omega},T)=\int_0^\infty\frac{g(\tau,T)\bar{\omega}d\tau}{1+\bar{\omega}^2\tau^2}\simeq\frac{\pi}{2}g\left(\frac{1}{\bar{\omega}},T\right) , \quad (5b)$$

$$m(\bar{\omega},T)=-\int_0^\infty\frac{\partial g(\tau,T)}{\partial\ln\tau}\frac{\bar{\omega}d\tau}{1+\bar{\omega}^2\tau^2} \simeq-\frac{\pi}{2}\left(\frac{\partial g(\tau,T)}{\partial\ln\tau}\right)_{\tau=1/\bar{\omega}} . \quad (5c)$$

The right-hand side of the equality (5c) is obtained by applying (4c) to (5b), and integrating by parts. The approximations in (5) are valid when $g(\tau,T)$ is broad in $\ln\tau$. Such fits of the spectra give $g(\tau,T)$ at the particular value $\tau=1/\bar{\omega}$, plus the integral (5a) and the derivative (5c).

The analysis assumes a broad distribution g. By fitting the spectra with $\kappa_R=1/(1+\omega^2\bar{\tau}^2)$ and $\kappa_I=\omega\bar{\tau}/(1+\omega^2\bar{\tau}^2)$ instead of (4), it can of course be checked whether a δ-function distribution is satisfactory. This was done in I, with negative results for strongly coupled spectra. Alternatively, having fitted using (4), one can check whether $\kappa_R/(\kappa_R^2+\kappa_I^2)\simeq 1$. That relation holds either for the δ-function distribution, or when the distribution weight is mostly at high frequencies ($\bar{\omega}\tau\ll 1$) so that $\kappa_R\simeq 1$ and $\kappa_I\simeq 0$. For a general distribution, the ratio becomes larger than 1 the more the distribution has weight at $\tau>1/\bar{\omega}$. Similarly, one can compare the measured value m to the expression $\kappa_R\kappa_I-\kappa_I^3/\kappa_R$. The latter should equal m only for the δ-function distribution.

Finally, when $g(\tau,T)$ can be expressed in terms of a function $f(E)$ of a single variable E, then the knowledge of $g(1/\bar{\omega},T)$ becomes sufficient to check the self-consistency of the values obtained for $\kappa_R(\bar{\omega},T)$, $\kappa_I(\bar{\omega},T)$, and $m(\bar{\omega},T)$. It is already known that the audio-frequency data can be collapsed in this manner if the single variable E is defined by (2).[15] Assuming this remains valid in the microwave region, one writes $g(\tau,T)d\ln\tau=f(E)dE$, which then gives $g(\tau,T)=(T-T_0)f(E)$. Using (5b), one obtains

$$f(\bar{E})=2\kappa_I(\bar{\omega},T)/\pi(T-T_0) , \quad (6)$$

where, $\bar{E}=(T-T_0)\ln(\omega_0/\bar{\omega})$. The values of the constants are $T_0\simeq 8.7$ K, and $\omega_0/2\pi\simeq 100$ cm^{-1}.[15] The self-consistency of $\kappa_R(\bar{\omega},T)$ is then checked using (5a) and (5b),

$$\kappa_R(\bar{\omega},T)=1-\frac{2}{\pi}\ln\left(\frac{\omega_0}{\bar{\omega}}\right)\int_T^\infty\frac{\kappa_I(\bar{\omega},T')}{(T'-T_0)}dT' . \quad (7a)$$

Similarly, the self-consistency of $m(\bar{\omega},T)$ is checked using (5b) and (5c),

$$\kappa_I(\bar{\omega},T)=(T-T_0)\ln\left(\frac{\omega_0}{\bar{\omega}}\right)\int_T^\infty\frac{m(\bar{\omega},T')}{(T'-T_0)^2}dT' . \quad (7b)$$

The T_1[100] spectra of I are now reanalyzed in this manner. Except for the new fit variables $\kappa_R(\bar{\omega},T)$, $\kappa_I(\bar{\omega},T)$, and $m(\bar{\omega},T)$, the procedure is identical to that in I. The data are taken over the broadest possible spectral range, i.e., from channel 20 upwards, in the notation of I, corresponding to $\omega_{\min}/2\pi\simeq 0.038$ cm^{-1}. For smaller shifts, the intensity of the elastically scattered light became significant in our setup. Spectra taken between 20 and 90 K were fitted. Outside this range, the coupling is much too small to extract reliable values. The χ^2's of all fits but two were smaller than one, with a mean value of $\simeq 0.68$ for all spectra.

The coefficients obtained are shown in Fig. 1. The error bars are statistical standard deviations. It is clear from Eq. (3) that systematic errors on Q or ω_a can seriously affect the coefficients, particularly κ_R. We estimate that this systematic error is at least as large as the statistical

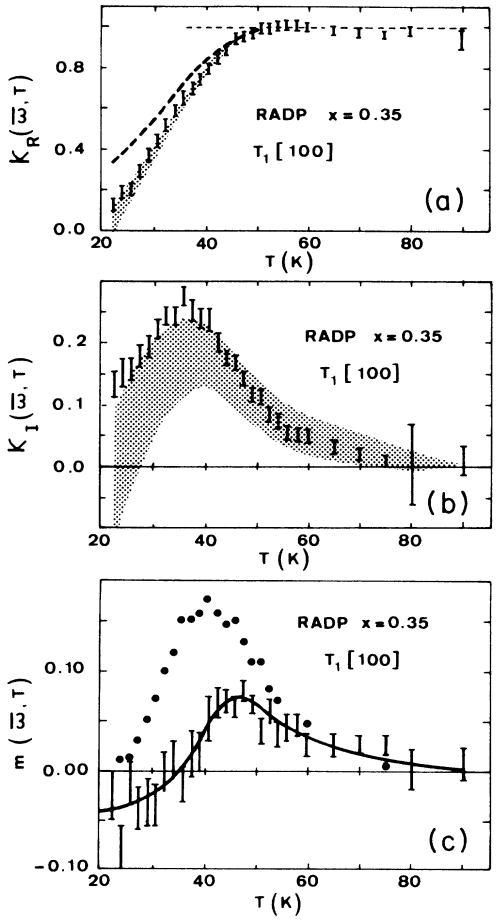

FIG. 1. Fit coefficients with their statistical error bars. (a) κ_R: The shaded area results from the integration of κ_I in (b) using (7a) with $T_0=8.7$ K. The dashed curve corresponds to the mean value of a similar calculation with $T_0=0$. The line at $\kappa_R=1$ is a guide to the eye. (b) κ_I: The shaded area results from the integration of m in (c) using (7b). (c) m: The solid curve is a guide to the eye. The open points are equal to $\kappa_R\kappa_I-\kappa_I^3/\kappa_R$ using values from (a) and (b).

error for κ_R, in particular below 35 and above 60 K. It was found empirically that the result for m is independent of the choice made for $\bar{\omega}$. Although m is rather poorly defined experimentally given our signal-to-noise ratio [resulting in the large error bars of Fig. 1(c)], it appears that m is truly a property of the measured spectra. The choice of $\bar{\omega}$ affects $\kappa_R(\bar{\omega})$ and $\kappa_I(\bar{\omega})$ so that the values of κ_R and κ_I calculated at $\omega=\omega_B$ using (4) are always reproduced. Since m is determined mostly by the spectral region between $\omega_{\min}$ and ω_B, the expansion was made about the intermediate value $\bar{\omega}/2\pi=0.10\ \mathrm{cm}^{-1}$.

The ratio $\kappa_R/(\kappa_R^2+\kappa_I^2)$ is checked in Fig. 2. Below 50 K, it grows above 1, indicating that the distribution acquires progressively more weight below $\bar{\omega}^{-1}$. This is clearly incompatible with a single Debye relaxation time. Similarly, m is compared to the experimental value of $\kappa_R\kappa_I-\kappa_I^3/\kappa_R$ [Fig. 1(c)]. The influence of the distribution is already seen below $\simeq 60$ K.

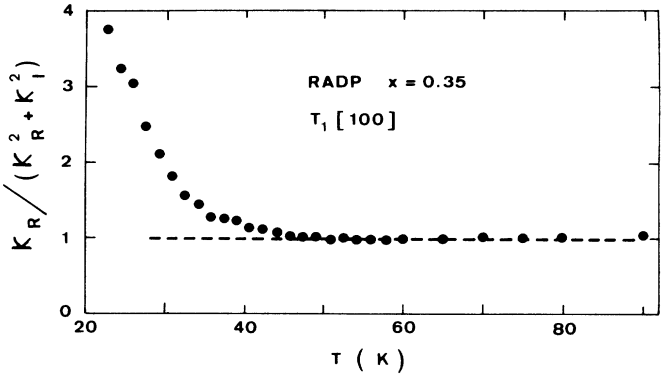

FIG. 2. The ratio $\kappa_R/(\kappa_R^2+\kappa_I^2)$, calculated from Figs. 1(a) and 1(b), demonstrates that, at low T, the distribution acquires weight at long times, $\tau > 1/\bar{\omega}$.

Second, the consequences of the VF ansatz (6) are checked. The distribution $f(\bar{E})$, derived from $\kappa_I(\bar{\omega},T)$ without adjustable parameter using (6), is shown in Fig. 3. The solid line is such that $\int f(\bar{E})d\bar{E}=1$. It is remarkable that this normalization does work, and that $f(E)$ is, in fact, quite similar to that obtained from audio-frequency data.[15] Identity of the two functions is not expected, as Ref. 15 is based on "free" dielectric data as opposed to "clamped" values here. Further, the self-consistency of the fit parameters can be checked. From m in Fig. 1(c), $\kappa_I(\bar{\omega},T)$ is calculated using (7b). The result is shown as the shaded area in Fig. 1(b). Its limits are obtained by integration of $m+\sigma$ and $m-\sigma$, respectively, where σ is the standard deviation on m. Although the agreement is not perfect, it can be considered as quite extraordinary for a no-free-parameter comparison and since m depends on minute details of the profiles. Integration of κ_I provides another check of the VF ansatz. It leads to the shaded area in Fig. 1(a), obtained using (7a). The agreement with κ_R is very good. This determination ap-

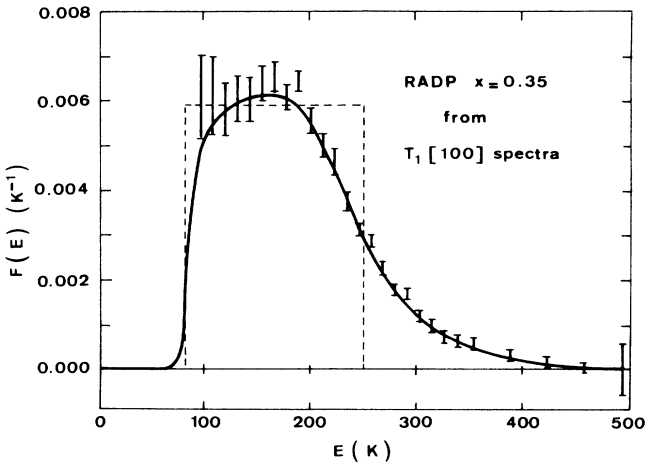

FIG. 3. The distribution $f(E)$ calculated from Fig. 1(b) using (6). The solid curve is a guide to the eye, and the dashed one illustrates the rectangular distribution approximation.

pears sufficiently accurate to allow checking the influence of T_0. The dashed curve on Fig. 1(a) corresponds to an Arrhenius law ($T_0=0$). It is seen that the VF ansatz gives a better agreement than the Arrhenius one.

In conclusion, it has been shown that coefficients of the expansion of the relaxation function in $\ln\omega$ can be derived from experimental spectra on model glasses. In the case of $Rb_{0.65}(NH_4)_{0.35}H_2PO_4$, those coefficients are consistent with the development of a broad distribution of relaxation times on cooling, and with a VF ansatz describing the scaling of the distribution with T. This new approach for the analysis of experimental data, which does not require the assumption of a particular shape for the distribution function, is expected to find rather broad application in the spectroscopy of glassy materials.

The Laboratoire de Science des Matériaux Vitreux is associated with the Centre National de la Recherche Scientifique (No. 1119).

[1]K. H. Fischer, Phys. Status Solidi (b) **130**, 13 (1985).
[2]K. Binder and A. P. Young, Rev. Mod. Phys. **58**, 801 (1986).
[3]L. Lundgren, P. Svedlindh, and O. Beckman, J. Magn. Magn. Mater. **25**, 33 (1981).
[4]L. E. Wenger, in *Proceedings of the Heidelberg Colloquium on Spin Glasses,* edited by L. Van Hemmen and I. Morgenstern (Springer, Berlin, 1983), p. 60.
[5]E. Pytte and Y. Imry, Phys. Rev. B **35**, 1465 (1987).
[6]Eric Courtens, Phys. Rev. Lett. **52**, 69 (1984); Eric Courtens and Hans Vogt, Z. Phys. B **62**, 143 (1986).
[7]Eric Courtens, J. Phys. (Paris) Lett. **43**, L199 (1982).
[8]E. Courtens and H. Vogt, J. Chim. Phys. **82**, 317 (1985).
[9]Eric Courtens, Jpn. J. Appl. Phys. **24**, Suppl. 2, 70 (1985); H. Terauchi, *ibid.* **24**, Suppl. 2, 75 (1985).
[10]Eric Courtens, René Vacher, and Yves Dagorn, Phys. Rev. B **33**, 7625 (1986).
[11]H. Vogel, Phys. Z. **22**, 645 (1921); G. S. Fulcher, J. Am. Ceram. Soc. **8**, 339 (1925).
[12]E. M. Brody and H. Z. Cummins, Phys. Rev. B **9**, 1979 (1974).
[13]One common method to bypass the problem is to use a sum of two δ functions. See, e.g., K. B. Lyons, P. A. Fleury, and D. Rytz, Phys. Rev. Lett. **57**, 2207 (1986).
[14]L. L. Landau and E. M. Lifshitz, *Statistical Physics* (Pergamon, London, 1958), Chap. XII.
[15]Eric Courtens, Phys. Rev. B **33**, 2975 (1986).